


 CrossMark  
click for updates

 Cite this: *Lab Chip*, 2015, 15, 504

## Hydrogen peroxide concentration by pervaporation of a ternary liquid solution in microfluidics†

Iwona Ziemecka,\* Benoît Haut and Benoit Scheid

Pervaporation in a microfluidic device is performed on liquid ternary solutions of hydrogen peroxide–water–methanol in order to concentrate hydrogen peroxide ( $\text{H}_2\text{O}_2$ ) by removing methanol. The quantitative analysis of the pervaporation of solutions with different initial compositions is performed, varying the operating temperature of the microfluidic device. Experimental results together with a mathematical model of the separation process are used to understand the effect of the operating conditions on the microfluidic device efficiency. The parameters influencing significantly the performance of pervaporation in the microfluidic device are determined and the limitations of the process are discussed. For the analysed system, the operating temperature of the chip has to be below the temperature at which  $\text{H}_2\text{O}_2$  decomposes. Therefore, the choice of an adequate reduced operating pressure is required, depending on the expected separation efficiency.

 Received 29th July 2014,  
Accepted 3rd November 2014

DOI: 10.1039/c4lc00886c

[www.rsc.org/loc](http://www.rsc.org/loc)

### 1. Introduction

Due to its strong oxidizing properties, hydrogen peroxide ( $\text{H}_2\text{O}_2$ ) is widely used in industry for bleaching, water treatment and therapeutic purposes. Most of its production is made through an optimized Riedl–Pfleiderer process,<sup>1</sup> the so-called anthraquinone process. This process allows the preparation of concentrated solution up to 70 wt% in  $\text{H}_2\text{O}_2$  but faces problems with effective quinone recycling and formation of by-products which have to be disposed. New applications such as medical tool sterilization or cleaning of microelectronic supports require highly concentrated  $\text{H}_2\text{O}_2$  solutions. However, the use of these solutions is only possible if they are produced on-site, as it is hazardous to transport  $\text{H}_2\text{O}_2$  solutions at concentrations higher than 30%. In that context, the on-site production of  $\text{H}_2\text{O}_2$  by direct synthesis using a microfluidic process has become an active research topic<sup>2,3</sup> as it is cost-effective, sustainable and offers the possibility to produce highly concentrated  $\text{H}_2\text{O}_2$  on demand. Moreover, such a microfluidic process would be an efficient laboratory tool, allowing for instance a rapid screening of operating conditions (pressure, temperature, nature of the catalyst, *etc.*) to increase the efficiency of the  $\text{H}_2\text{O}_2$  production reaction with the use of a limited amount of reactants and catalysts.

Ideally, a microfluidic process for  $\text{H}_2\text{O}_2$  production would be composed of a chip with interconnected modules dedicated to the production of  $\text{H}_2\text{O}_2$  and its purification. One of the crucial modules in such a microfluidic process is to obtain, after the reaction, concentrated  $\text{H}_2\text{O}_2$  by separating it from the other liquid components (by-products and solvents) present in the process. Pervaporation in a microfluidic device seems to be a good method for such a separation as explained below.

Pervaporation is a membrane separation process that is an energy-efficient combination of permeation and evaporation.<sup>4</sup> It is used to remove volatile compounds out of solutions. By creating a vacuum (vacuum pervaporation) or introducing a flow of inert gas (purge gas pervaporation) on one side of a dense (non-porous) membrane, volatile compounds in a liquid flow on the other side of the membrane will tend to diffuse through this membrane.

Purge gas pervaporation microfluidic devices were used to concentrate various aqueous solutions *via* pervaporation of water through a PDMS membrane in order to study phase diagrams, either steady or out of equilibrium,<sup>5</sup> or the kinetics of such a pervaporation process.<sup>6</sup> In these studies, binary aqueous solutions were considered.

Separation methods similar to pervaporation were already investigated for several liquid solutions using different types of microfluidic devices.<sup>7–9</sup> Hartman *et al.*<sup>7</sup> used distillation in microfluidics for binary organic solution separation. Their device consisted of a capillary in which vapour–liquid equilibrium was reached using segmented flow and a porous membrane to separate the vapour and the liquid flows using capillary forces. Zhang *et al.*<sup>8</sup> designed a multi-layered chip

TIPs, Ecole Polytechnique de Bruxelles, ULB, CP165/67, Avenue F.D. Roosevelt 50, 1050 Bruxelles, Belgium. E-mail: Iwona.Ziemecka@ulb.ac.be;

Fax: +32 2 650 29 10; Tel: +32 2 650 29 16

† Electronic supplementary information (ESI) available. See DOI: 10.1039/c4lc00886c

for vacuum distillation of  $\text{H}_2\text{O}$ – $\text{MeOH}$  solutions using a temperature gradient. In the work of Adiche and Sundmacher,<sup>9</sup> the distillation of  $\text{H}_2\text{O}/\text{MeOH}$  solutions in microfluidics was studied with the use of different porous membranes.

Because gaseous  $\text{H}_2$  and  $\text{O}_2$ , the reagents for the production of  $\text{H}_2\text{O}_2$ , have a higher solubility in liquid methanol ( $\text{MeOH}$ ) than in water, we foresee that the next generation of chips for the direct synthesis of  $\text{H}_2\text{O}_2$  will involve the use of  $\text{MeOH}$  as a co-solvent (with  $\text{H}_2\text{O}$ ). After reaction,  $\text{H}_2\text{O}_2$  and  $\text{H}_2\text{O}$  will have to be separated from  $\text{MeOH}$  which is undesirable for some applications but still tolerated at very low concentrations of about 1%.

In the present manuscript, we report the use of a microfluidic chip for the concentration of  $\text{H}_2\text{O}$  using pervaporation in ternary solutions of  $\text{H}_2\text{O}_2$ ,  $\text{MeOH}$  and  $\text{H}_2\text{O}$ . These liquid solutions are processed through a chip designed and developed in our lab. This chip is built as a multi-layer device, as represented in Fig. 1. The key element of this device is the dense membrane<sup>10</sup> situated in-between a liquid channel and a vapour channel in contact, respectively, with a cooling and a heating plate. The liquid solution flows through the liquid channel and the different components of the solution can diffuse through the membrane to reach the vapour channel. According to the relative volatility of the components considered in this work, such a system should allow  $\text{H}_2\text{O}_2$  to concentrate in the liquid solution.

We first present the materials and methods (section 2). As compared to previous studies of the separation in microfluidics, no segmented flows in the liquid channel or inert gas flows in the vapour channel are used, and our setup combines vacuum and a temperature gradient as driving forces for the diffusion through the membrane. To the best of our knowledge, it is the first example of a microfluidic device where the pervaporation of a liquid ternary solution is analysed and it is the first attempt of concentration of a solution containing  $\text{H}_2\text{O}_2$  using microfluidic technology.

A quantitative analysis using nuclear magnetic resonance (NMR) of the composition of the phases† exiting the chip is realized for various operating temperatures of the chip and

various compositions of the liquid solution introduced in the chip. Experimental results together with a mathematical model of the process are then used to understand the effect of the operating conditions on the separation process efficiency (section 3). The parameters influencing significantly the performance of the pervaporation in the chip are determined and the limitations of the process are discussed (section 4). Finally, the conclusions are addressed (section 5).

## 2. Materials and methods

### 2.1 Materials

$\text{MeOH}$  (HPLC grade) and a liquid solution of  $\text{H}_2\text{O}_2$  (30 wt%) in  $\text{H}_2\text{O}$  were purchased from Sigma-Aldrich. Hexamethyldisilazane was purchased from Fluka Analytical. They were used as received. A liquid solution of  $\text{H}_2\text{O}_2$  (60 wt%) in  $\text{H}_2\text{O}$  was received from Solvay company. Polydimethylsiloxane (PDMS) was prepared from Sylgard 184, Dow Corning.

### 2.2 Preparation of the microfluidic device

Fabrication of the device is performed using soft lithography. Two 4-inch silicon wafers are patterned by exposing a layer of photoresist resin (SU8-2150, MicroChem) to UV light using the UV-KUB-2 insulator from Kloé company through a high-resolution transparency mask containing the two-dimensional designs of the microchannel circuits (one for the liquid channel and one for the vapour channel). These patterned wafers are subsequently used as a mold to replicate the structure in the PDMS layer of 4 mm thickness. Our device is built up from two layers of PDMS, sandwiching a PDMS membrane, which are prepared using a mixture of pre-polymer and a curing agent in a 5 : 1 ratio by weight and cured at 70 °C for 2 hours for high cross-linking. The layers are bonded to the membrane after 30 s exposure in a plasma chamber (Harrick).

### 2.3 Preparation of the membrane

The PDMS membrane is prepared by spin-coating a PDMS (pre-polymer and curing agent in a 10 : 1 ratio by weight) layer on a silicon wafer silanized with hexamethyldisilazane and baked at 70 °C for 2 hours. The membrane thickness of 170  $\mu\text{m}$  is measured with a Keyence VK-X200 3D laser microscope. It is a dense membrane, permeable to  $\text{H}_2\text{O}$ ,  $\text{H}_2\text{O}_2$ , and  $\text{MeOH}$ .<sup>10–13</sup> According to Bell *et al.*,<sup>12</sup> the permeability coefficients for  $\text{H}_2\text{O}$  and  $\text{MeOH}$  in PDMS are of comparable values. Furthermore, the permeability of  $\text{H}_2\text{O}_2$  is assumed to be identical to the permeability of  $\text{H}_2\text{O}$ . Consequently, it is the relative volatility of these three components that is responsible for the efficiency of the separation process using the microfluidic device.

### 2.4 Building of the chip

Membranes with different compositions (PTFE,<sup>8</sup> PES, and PVDF) were previously tested for membrane distillation of  $\text{MeOH}/\text{H}_2\text{O}$  solutions.<sup>9</sup> In the microdevices described, membranes were incorporated and fixed by mechanical screwing,

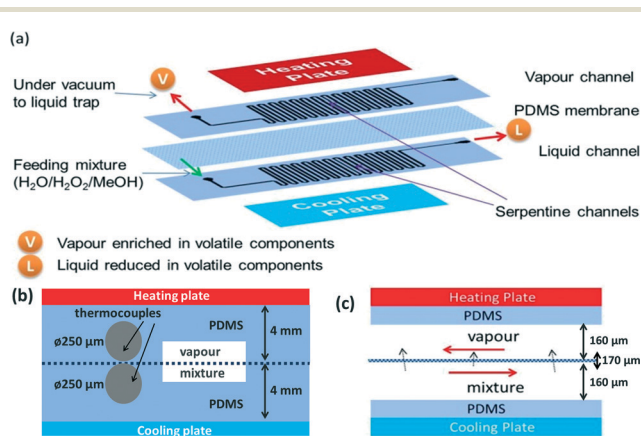


Fig. 1 Scheme of the device: (a) general overview, (b) cross section, (c) side view. Sketches are not to scale.

which caused the problem of leakage. In our setup, we use a membrane made of PDMS as it is commonly used in micro-engineering.<sup>10</sup> Since our microchannels are also imprinted within PDMS, it allows a tight and hermetic connection with the membrane through plasma bonding. The compatibility of PDMS with MeOH solution has also been tested in our work and elsewhere.<sup>14</sup>

Dimensions of the microchannels have to be carefully chosen to ensure an efficient mass transfer of the most volatile compound from the liquid channel to the vapour channel. The liquid channel has a width of 300  $\mu\text{m}$  and the vapour channel has a width of 500  $\mu\text{m}$ . This size difference guarantees that the vapour channel entirely overlaps the liquid channel. With this approach, we prevent the formation of dead zones (due to misalignment), *i.e.* areas where there is no exchange possible through the membrane from the liquid to the vapour channel. A careful alignment of the vapour channel with the liquid channel is required and it is achieved in such a way that the bottom layer (with the liquid channel) is first bonded to the PDMS membrane. Then, the top PDMS layer (with the vapour channel) is bonded to the other side of the membrane.

The liquid solution of  $\text{H}_2\text{O}$ , MeOH and  $\text{H}_2\text{O}_2$  is injected within the liquid channel with the help of a syringe pump, whereas partial vacuum is applied to the vapour channel allowing the collection of the vapour condensate within a trap dipped in ice. Flows in microchannels are generally laminar, which means that solvent molecules can only move in a direction transverse to the direction of the flow by diffusion. Based on the diffusion coefficient of MeOH (most volatile component) in  $\text{H}_2\text{O}$  ( $1.014 \times 10^{-9} \text{ m}^2 \text{ s}^{-1}$  at 25 °C for 0.28 mole fraction of MeOH),<sup>8</sup> we deduced that the liquid microchannel, which is 160  $\mu\text{m}$  high, 300  $\mu\text{m}$  wide and 90 cm long, ensures that at a flow rate of 0.1  $\mu\text{L s}^{-1}$ , the process is not limited by diffusion in the liquid channel, the mixing length being about 5 cm.

At the exit of the liquid channel, a more concentrated solution in  $\text{H}_2\text{O}_2$  should be obtained compared to the liquid solution introduced in the chip. Quantification of the concentration in each component is realized by NMR spectroscopy. The composition of the collected condensed vapour is determined to show, on the one hand, what the concentration in each component is and to ensure, on the other hand, that nothing is lost during the process through PDMS walls.

Temperatures ranging from 70 to 90 °C inside the chip are considered for our set of experiments. Indeed, it has been shown that at higher temperature, decomposition of  $\text{H}_2\text{O}_2$  occurs.<sup>17</sup>

## 2.5 Chip operation

The liquid solution is introduced in the liquid channel with the use of a syringe pump at a flow rate of 0.1  $\mu\text{L s}^{-1}$ . The vapour channel is connected to a vacuum pump and a negative pressure of -500 mbar is applied. This is for the purpose of pumping the vapour from the vapour channel in

a direction opposite to the flow direction in the liquid channel (see Fig. 1).

## 2.6 Temperature control

A Peltier element (Thermo Electric Module TES1 12703S, 27 W, 14.5 V, BTS Europe BV) is used as a cooling system. The cold side of the Peltier element is directly put in contact with the PDMS layer containing the liquid channel. To dissipate the heat, the hot side of the Peltier element is glued to an aluminium plate connected to a water cooling system. A heating resistor (24 V, 40 W, 14.5  $\Omega$ , GBR-666/24/1, TELPOD) is used as a heating device. It is glued to an aluminium plate that is in contact with the PDMS layer containing the vapour channel. The heating plate is positioned on top of the vapour channel such that condensation of the vapour does not occur within the channel. It also ensures an efficient temperature gradient through the chip due to the cooling plate located underneath the liquid channel. It is noticed that both temperature elements are only covering the serpentes (see Fig. 1). As mentioned hereafter, only the measurement of the temperature in the liquid channel is needed for the comparison between the experimental data and the model presented in section 3.

We measure precisely the temperature inside the chip with the use of 0.25 mm diameter thermocouples (Omega, TJ36-CASS-010G-12). The thermocouples are placed at different places along the liquid and vapour channels. No temperature gradient along the channels is observed, at least within the error of the thermocouples ( $\pm 1$  °C). The temperature difference between the liquid channel and the vapour channel is measured to be 2 °C for the range of temperatures considered. There can be some inaccuracy in the determination of the temperature in the channels, since the thermocouples are not exactly inside the channels (see Fig. 1) and also since the thermocouple diameter is 0.25 mm, *i.e.* larger than the height of the microchannel (0.16 mm).

## 2.7 Quantitative analysis

NMR is used to characterize the composition of the output phases of the microfluidic device (Fig. S1–S3†).  $\text{H}_2\text{O}_2$  can be characterized by NMR in acetone at low concentrations.<sup>14</sup> For our present measurements, 10  $\mu\text{L}$  of the extracted solution is diluted in 590  $\mu\text{L}$  of acetone- $d_6$ . Measurements are performed at -25 °C using a 600 MHz Varian instrument. The analysed solutions had a pH around 6. With these conditions, good separation of the signals inherent to  $\text{H}_2\text{O}_2$ ,  $\text{H}_2\text{O}$  and MeOH is obtained. The error of NMR measurement is 5%.

## 3. Mathematical model

A coordinate  $x$  along the microchannels is introduced. The value of  $x$  is 0 at the inlet of the liquid channel (and hence at the outlet of the vapour channel) and  $x$  equals  $L_p$  at the outlet of the liquid channel (and hence at the dead end of the

vapour channel). For our chip,  $L_p = 0.9$  m. For reasons explained hereafter, a flow of inert gas is considered in the developed mathematical model of the chip. This inert gas is introduced in the chip at  $x = L_p$  and flows with the generated vapour towards  $x = 0$ . The parameter  $L(x)$  ( $\text{mol s}^{-1}$ ) is the molar flow rate of liquid at position  $x$  in the liquid channel. The parameter  $G(x)$  ( $\text{mol s}^{-1}$ ) is the molar flow rate of gas at position  $x$  in the vapour channel. The molar fractions of  $\text{H}_2\text{O}$ , MeOH and  $\text{H}_2\text{O}_2$  in the liquid at position  $x$  in the liquid channel are written as  $w_l(x)$ ,  $m_l(x)$  and  $h_l(x)$ , respectively. The molar fractions of inert gas,  $\text{H}_2\text{O}$ , MeOH and  $\text{H}_2\text{O}_2$  in the gas at position  $x$  in the vapour channel are written as  $i_g(x)$ ,  $w_g(x)$ ,  $m_g(x)$  and  $h_g(x)$ , respectively.

The following balance equations can be written:

$$w_l(x) + m_l(x) + h_l(x) = 1 \quad (1)$$

$$i_g(x) + w_g(x) + m_g(x) + h_g(x) = 1 \quad (2)$$

$$\frac{d}{dx}(L(x)w_l(x)) = -WJ_w(x) \quad (3)$$

$$\frac{d}{dx}(L(x)m_l(x)) = -WJ_m(x) \quad (4)$$

$$\frac{d}{dx}(L(x)h_l(x)) = -WJ_h(x) \quad (5)$$

$$\frac{d}{dx}(G(x)w_g(x)) = -WJ_w(x) \quad (6)$$

$$\frac{d}{dx}(G(x)m_g(x)) = -WJ_m(x) \quad (7)$$

$$\frac{d}{dx}(G(x)h_g(x)) = -WJ_h(x) \quad (8)$$

$$\frac{d}{dx}(G(x)i_g(x)) = 0 \quad (9)$$

where  $W$  ( $=300 \mu\text{m}$  for our chip) is the width of the liquid channel and  $J_w(x)$ ,  $J_m(x)$  and  $J_h(x)$  are the molar fluxes ( $\text{mol s}^{-1} \text{m}^{-2}$ ) of  $\text{H}_2\text{O}$ , MeOH and  $\text{H}_2\text{O}_2$  across the membrane at position  $x$ , respectively. According to Bell *et al.*<sup>12</sup> and using Raoult's equations, these fluxes can be expressed as follows:

$$J_w(x) = \frac{P_w}{H}(w_l(x)P_{\text{sat,w}}(T) - w_g(x)P) \quad (10)$$

$$J_m(x) = \frac{P_m}{H}(m_l(x)P_{\text{sat,m}}(T) - m_g(x)P) \quad (11)$$

$$J_h(x) = \frac{P_h}{H}(h_l(x)P_{\text{sat,h}}(T) - h_g(x)P) \quad (12)$$

where  $H$  ( $=170 \mu\text{m}$  for our chip) is the thickness of the

membrane,  $P$  ( $=500$  mbar in our experiments) is the pressure in the vapour channel and  $T$  is the temperature in the liquid channel;  $P_w$ ,  $P_m$  and  $P_h$  are the permeability coefficients of liquid  $\text{H}_2\text{O}$ , MeOH and  $\text{H}_2\text{O}_2$  across the membrane, respectively. According to Bell *et al.*,<sup>12</sup>  $P_w$  and  $P_m$  are, at ambient temperature, close to  $\exp(-25) \text{mol m}^{-1} \text{s}^{-1} \text{Pa}^{-1}$ .  $P_{\text{sat,w}}(T)$ ,  $P_{\text{sat,m}}(T)$  and  $P_{\text{sat,h}}(T)$  are the saturation pressures of  $\text{H}_2\text{O}$ , MeOH and  $\text{H}_2\text{O}_2$ , respectively. They are expressed as a function of  $T$  as follows:

$$P_{\text{sat,w}}(T) = 101325 \text{e}^{\frac{13.7 - \frac{5120}{T+273.15}}{}} \quad (13)$$

$$P_{\text{sat,m}}(T) = 13310 \text{e}^{\frac{8.8 - \frac{2002}{T+273.15}}{}} \quad (14)$$

$$P_{\text{sat,h}}(T) = \text{e}^{4.6+0.051 T} \quad (15)$$

where  $T$  is in  $^\circ\text{C}$  and the pressures are in Pa. Eqn (12) and (13) are given in Lange's Handbook of Chemistry,<sup>15</sup> and eqn (14) has been derived from data provided in a paper by J. J. van Laar<sup>16</sup> and is valid for  $T$  between 50 and 100  $^\circ\text{C}$ .

The molar flow rate of liquid introduced in the chip is written as  $L_0$  ( $\text{mol s}^{-1}$ ). The molar fractions of  $\text{H}_2\text{O}$ , MeOH and  $\text{H}_2\text{O}_2$  in this liquid are written as  $w_0$ ,  $m_0$  and  $h_0$ , respectively. The following boundary conditions complete the balance equations:

$$L(0) = L_0, m_l(0) = m_0, h_l(0) = h_0, \quad (16)$$

$$G(L_p) = r L_0, m_g(L_p) = \varepsilon, h_g(L_p) = \varepsilon, i_g(L_p) = 1 - 3\varepsilon \quad (17)$$

Eqn (1)–(17) compose the mathematical model of the separation process. The introduction of an inert gas in the vapour channel at  $x = L_p$  is considered in this model in order to avoid undetermined values for  $m_g(x)$  and  $h_g(x)$  at  $x = L_p$ . After eliminating  $i_g(x) = r L_0(1 - 3\varepsilon)/G(x)$  by solving (9) with (17), this model allows predicting the composition of the outlet phases ( $w_l(L_p)$ ,  $m_l(L_p)$ ,  $h_l(L_p)$ ,  $w_g(0)$ ,  $m_g(0)$ ,  $h_g(0)$ ) and the outlet fluxes ( $L(L_p)$ ,  $G(0)$ ), *i.e.* 8 unknowns, as functions of  $L_p$ ,  $H$ ,  $W$ ,  $T$ ,  $P$ ,  $L_0$ ,  $w_0$ ,  $m_0$  and  $h_0$ . This algebraic-differential system of eqn (1)–(8) is solved as a boundary-value problem using continuation software AUTO-07p.<sup>19</sup> In order for the solutions to be compared with the experimental results, they are solved for  $\varepsilon \rightarrow 0$  and  $r \rightarrow 0$ . In practice we have used  $\varepsilon = 10^{-6}$  and  $r = 10^{-3}$ , for which the solutions were found to be independent of these parameters.

## 4. Results and discussion

Inoue *et al.*<sup>2,3</sup> have produced 3 wt% to 10 wt%  $\text{H}_2\text{O}_2$  solutions by direct synthesis from hydrogen ( $\text{H}_2$ ) and oxygen ( $\text{O}_2$ ) in a microfluidic device. This reaction proceeded in  $\text{H}_2\text{O}$  with the use of different catalysts (mostly palladium).

As mentioned previously, we foresee that the next generation of direct synthesis of  $\text{H}_2\text{O}_2$  in microfluidic chips will

involve the use of MeOH as co-solvent. Three different liquid solutions are introduced in the chip with different compositions: (i)  $w_0 = 0.63$ ,  $m_0 = 0.35$ ,  $h_0 = 0.02$ ; (ii)  $w_0 = 0.61$ ,  $m_0 = 0.33$ ,  $h_0 = 0.06$ ; and (iii)  $w_0 = 0.15$ ,  $m_0 = 0.74$ ,  $h_0 = 0.11$ . The chip is operated at different temperatures. These different compositions and temperatures are used to understand the effect of the operating conditions on the separation process efficiency. It can be calculated that the mass fraction of  $H_2O_2$  in the liquid solutions introduced in the chip is between 3.3 and 12, thus covering the range of mass fractions produced by Inoue *et al.*<sup>2</sup> The experiments were repeated three times for each temperature and each inlet composition. In Fig. 2, the collected experimental data, *i.e.* molar fractions of  $H_2O_2$ ,  $H_2O$  and MeOH, at the outlets of the chip, in the liquid and the vapour phases, are presented and compared to the model results (using values of  $P_w$  and  $P_m$  obtained by Bell *et al.*,<sup>12</sup> at ambient temperature and assuming  $P_h = P_w$ ). It is important to mention here that to use the model, the temperature  $T$  in the liquid channel has to be defined and there is an uncertainty in the experimental determination of  $T$  inside the channels for the reasons explained in section 2.6.

After processing through the chip and for any of the liquid solutions used,  $H_2O_2$  was concentrated and the MeOH concentration was decreased in the liquid phase. The experimental data presented in Fig. 2(b) shows that at 85 °C, the  $H_2O_2$  concentration in the liquid phase is doubled from  $h_0 = 0.02$  to  $h_1(L_p) = 0.04$  and that the MeOH concentration in the liquid phase is decreased by a factor of four from  $m_0 = 0.35$  to  $m_1(L_p) = 0.08$ . Furthermore, only very small amounts (traces) of  $H_2O_2$  are detectable in the vapour phase produced. It is an obvious consequence of the low volatility (compared to  $H_2O$  and MeOH) of  $H_2O_2$  at the considered temperatures. The experimental results presented here thus demonstrate that the developed chip can be successfully operated to separate MeOH and  $H_2O_2$  to a certain extent. The maximum obtained concentration of  $H_2O_2$  in the liquid outlet is close to 30 wt% (molar fraction of 0.2).

A mass balance realized on the experimental results highlights that at high operating temperatures in the chip (above 85 °C), the amount of  $H_2O_2$  leaving the chip is significantly smaller than the amount of  $H_2O_2$  entering the chip. This behaviour was expected as it is commonly known that

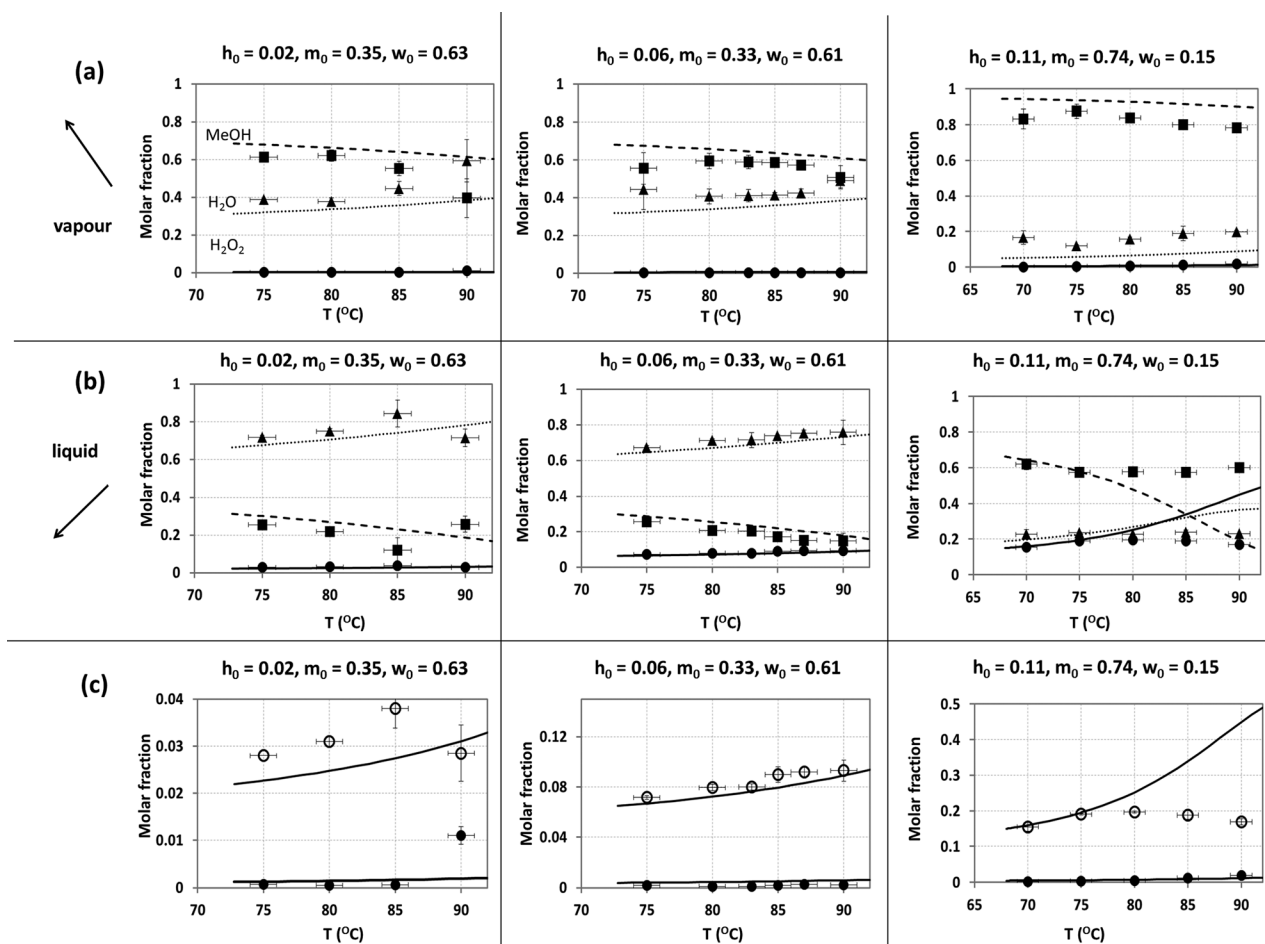


Fig. 2 Comparison of experimental results (symbols) and theoretical results (lines) for pervaporation of three different compositions of  $H_2O_2/H_2O/MeOH$  mixtures at different temperatures. (a) Outlet vapour phase, (b) outlet liquid phase, (c)  $H_2O_2$  in vapour (black circles) and liquid phase (open circles). Squares and dashed lines: MeOH, triangles and dotted lines:  $H_2O$ , circles and solid lines:  $H_2O_2$ .

an increase in the temperature favours the process of decomposition of  $\text{H}_2\text{O}_2$ .<sup>17</sup> Additionally, the liquid solutions introduced in the chip as well as the collected condensed vapours have a pH around 6, which is not optimum for the storage of  $\text{H}_2\text{O}_2$ ; a pH below 5 is preferred.<sup>18</sup> On the other hand, mass balances for experiments performed with temperature below 85 °C highlight no significant decomposition of  $\text{H}_2\text{O}_2$ . The vapour channel, which is the part of the device that is exposed to the highest temperature, is connected to vacuum. It highly decreases the time during which  $\text{H}_2\text{O}_2$  is exposed to high temperature. This probably contributes to the very small  $\text{H}_2\text{O}_2$  decomposition for  $T < 85$  °C. For the above-mentioned reasons, a temperature of 85 °C or lower should be used for the process of any  $\text{H}_2\text{O}_2/\text{H}_2\text{O}/\text{MeOH}$  liquid solution in the chip. In our experiments we do not observe significant escape of MeOH through the walls of the PDMS chip. This observation was verified by mass balances as detailed in the ESI.† PDMS is permeable to gases but we expect that due to the applied negative pressure in the vapour channel and to the thick and highly cross-linked PDMS walls, escape of MeOH should be prevented.

We thus conclude that PDMS layers and PDMS membrane are compatible with the system used at all working temperatures.

When the collected outlet phases are characterized by NMR, no additional signal from the dissolution of PDMS by the used mixtures is detectable (see, for example, Fig. S1 in the ESI†). We also found that no additional NMR signal was observed in a water solution of 50%  $\text{H}_2\text{O}_2$  in which a piece of PDMS has been boiled for 1 h. Pervaporation was also carried out in an analog chip made of NOA 81 (Norland Optical Adhesives), which is known to be not permeable to gases, but when pervaporation is performed at high temperature unexpected additional NMR signals in NMR spectra are observed probably caused by the dissolution of NOA.

Although our PDMS microfluidic device with a PDMS membrane has good compatibility with the processed solutions and shows no leakage issue, different materials can be used to make a chip with, for instance, the use of a selective membrane. Careful choice has to be made to prevent leakage which is often the problem for membranes in chips. In our case such a problem was not detected.

Yet, the geometry of the chip can still be investigated and improved. The use of segmented flow (by injecting nitrogen bubbles for instance) can improve the vapour transfer to the vapour channel which can result in decreasing the operating temperature and thus preventing the degradation of  $\text{H}_2\text{O}_2$ .

A good agreement between the experimental data and the mathematical model is obtained except at high temperature (above 85 °C). The discrepancies between the model and the experimental data are caused by different factors, which we discuss below.

First, as mentioned previously, there is an uncertainty on the values of  $T$  due to measurement inaccuracy that have to be used in the model for an adequate comparison with the experimental data.

Second, the decomposition of  $\text{H}_2\text{O}_2$  at high temperature is not taken into account in the model. This contributes

probably to the fact that the deviation between the experimental data and the model increases when the temperature inside the chip increases and is typically larger than 85 °C. This is clearly observed in Fig. 2 (right column).

Third, the expressions of  $J_w(x)$ ,  $J_m(x)$  and  $J_h(x)$  are based on the use of Raoult's equations. These equations are only valid for ideal solutions, which is not strictly our case.

Fourth, the values of  $P_w$ ,  $P_m$  and  $P_h$  used in the model were obtained by other authors (using an unspecified concentration of the curing agent for the PDMS membrane) and are considered independent of the temperature. To increase the accuracy of the model, these permeability coefficients should be determined experimentally at different temperatures for the membrane used in this work.

To conclude, based on this analysis we foresee that the biggest discrepancy will be obtained at the highest temperature and for the solution containing the highest concentration of  $\text{H}_2\text{O}_2$ . This solution is the furthest from ideal so the vapour pressure obtained using Raoult's equations and used in our model will be the most different from the true vapour pressure.

Nevertheless, it is not our intention to provide a more complex description of the vapour-liquid equilibrium of the solutions to model the studied process, but rather to provide a simple model that allows grasping the general behaviour of the system and identifying the relevant key parameters. In that spirit, the correspondence between the model and the experimental data seems reasonable.

Yet, the model can be used to characterize qualitatively the operation of the chip. For this purpose, three efficiencies of the chip are defined:

$$\eta_1 = 1 - \frac{L(L_p)m_1(L_p)}{L_0m_0} \quad (18)$$

$$\eta_2 = \frac{L(L_p)h_1(L_p)}{L_0h_0} \quad (19)$$

$$\eta_3 = \eta_1 \eta_2 \quad (20)$$

The efficiency  $\eta_1$  quantifies the transfer of the MeOH from the liquid channel to the vapour channel. The value  $\eta_1 = 1$  means that the MeOH introduced in the chip has been entirely transferred to the vapour channel. The efficiency  $\eta_2$  quantifies the conservation of  $\text{H}_2\text{O}_2$  in the liquid channel. The value  $\eta_2 = 1$  means that no  $\text{H}_2\text{O}_2$  has been transferred in the vapour channel. The parameter  $\eta_3$  can be seen as an overall efficiency of the chip that is equal to 1 only when  $\eta_1$  and  $\eta_2$  are equal to 1.

In order to avoid the decomposition of  $\text{H}_2\text{O}_2$ , it is important to work at a maximum temperature of 85 °C. If the objective of the operation of the chip is to remove almost the entire amount of methanol in the liquid phase ( $\eta_1 \rightarrow 1$ ), the operating pressure of the chip should be selected such that even a pure methanol vapour phase leaving the chip could not be in equilibrium with the inlet liquid solution regarding

the mass transfer of methanol through the membrane ( $J_m(0) > 0$ ). If this condition is fulfilled, any increase in the channel length  $L_p$  would lead to an increase in the amount of methanol transferred from the liquid to the vapour. According to eqn (11), this condition can be simply written as  $m_0 P_{\text{sat,m}}(T) > P$ . For  $m_0 = 0.33$  (the lowest considered value of  $m_0$  in our experiments) and  $T = 85$  °C, this condition is equivalent to  $P < 712$  mbar, which is actually fulfilled in our setup. This highlights the importance of working at a reduced pressure according to the composition of the liquid inlet.

Using the model,  $\eta_1$ ,  $\eta_2$  and thus  $\eta_3$  can be calculated as a function of  $L_p$ . For instance, for a liquid solution corresponding to the second set of our experiments ( $w_0 = 0.61$ ,  $m_0 = 0.33$ ,  $h_0 = 0.06$ ) and for  $W = 300$   $\mu\text{m}$ ,  $H = 170$   $\mu\text{m}$ ,  $P = 500$  mbar,  $T = 85$  °C,  $\eta_1$  and  $\eta_2$  are presented in Fig. 3 as a function of  $L_p$ . It can be seen that the performance of the chip can be strongly enhanced for longer channels. For instance, if  $L_p = 4$  m,  $\eta_1 = \eta_2 = 0.94$ , meaning that for the considered liquid solution, 94% of the MeOH introduced in the chip could be transferred to the vapour channel, while 94% of the  $\text{H}_2\text{O}_2$  introduced in the chip would remain in the liquid channel.

The model can also be used to calculate the values of  $\eta_1$ ,  $\eta_2$  and  $\eta_3$  that would be obtained in a chip operated with a vapour outflow at  $x = L_p$  (co-current flows) instead of at  $x = 0$  (countercurrent flows). For this purpose, the minus signs appearing in eqn (6–8) have to be replaced by plus signs and the boundary conditions (17) have to be written at  $x = 0$ . Every other parameter of the system being the same, calculations show that the efficiencies obtained in the case of countercurrent flows are higher than the efficiencies obtained in the case of co-current flows. This is a consequence of the fact that as it is well known in chemical engineering, countercurrent flows offer a higher average driving force for heat and mass transfers than co-current flows. Therefore, while in the case of Fig. 3 the overall efficiency  $\eta_3$  is found to continuously increase with  $L_p$  for the countercurrent flows up to 10 m, it passes by a maximum at 3 m for the co-current flows, where  $\eta_3 = 0.75$ . Beyond 3 m,  $\eta_2$  decreases quickly meaning that a large amount of  $\text{H}_2\text{O}_2$  is then going to the

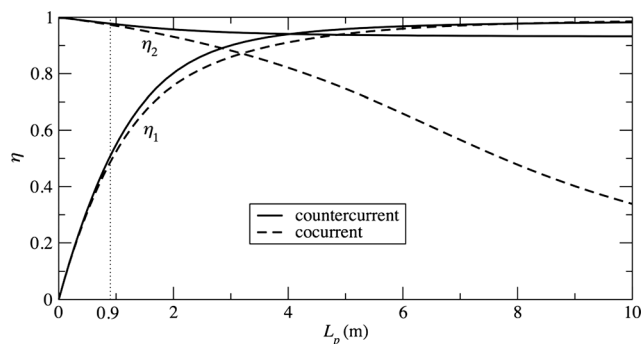


Fig. 3 Efficiencies of the chip as a function of  $L_p$ . Continuous line: chip operated with countercurrent flows, dashed lines: chip operated with co-current flows.  $w_0 = 0.61$ ,  $m_0 = 0.33$ ,  $h_0 = 0.06$ ,  $W = 300$   $\mu\text{m}$ ,  $H = 170$   $\mu\text{m}$ ,  $P = 500$  mbar and  $T = 85$  °C. The dotted line indicates the outlet of the channel used in the experiments.

vapour phase, reducing drastically the capacity of the chip to concentrate  $\text{H}_2\text{O}_2$  in the case of co-current flows.

## 5. Conclusions

We successfully designed and operated a chip for the pervaporation of  $\text{H}_2\text{O}_2/\text{H}_2\text{O}/\text{MeOH}$  ternary mixtures in order to concentrate  $\text{H}_2\text{O}_2$  by removing MeOH. Even if solutions with a low amount of  $\text{H}_2\text{O}_2$  have been considered up to now (the maximum obtained concentration of  $\text{H}_2\text{O}_2$  in the liquid outlet is close to 30 wt%), this work can be seen as a proof of concept and is the first step towards the design of a purification chip meeting the industrial requirements. We show that  $\text{H}_2\text{O}_2$  can be successfully concentrated and MeOH removed to some extent already in a single chip. Technology and technical issues have been tackled and solutions described. Advantages and disadvantages of the chip have been discussed and further improvement proposed. A model of the chip has been developed and compared successfully with experimental data. The discrepancies between the model and the experimental results are discussed. Such a model could allow, based on the composition of the liquid solution that should be processed, the design of a chip to fulfill a given requirement.

The combined analysis of the experimental results and the model allows highlighting the key phenomena governing the operation of the chip. A significant thermal decomposition of  $\text{H}_2\text{O}_2$  appears to occur at temperature above 85 °C. Such temperature should thus be avoided. If the objective of the operation of the chip is to remove almost the entire amount of methanol in the liquid phase ( $\eta_1 \rightarrow 1$ ), the operating pressure of the chip should be carefully selected such that even a pure methanol vapour phase leaving the chip could not be in equilibrium with the inlet liquid solution, regarding the mass transfer of methanol through the membrane. Using the model, it is also demonstrated that a chip with countercurrent vapour and liquid flows present higher efficiencies than a chip that would be operated with concurrent flows.

It is worth noting that the developed model does not contain any unknown value. No fit is realized and the used values for the permeability are obtained from the literature.

To increase the accuracy of the model, the permeability coefficients of the membrane used in this work should be determined experimentally at different temperatures. It would be also interesting to analyse the influence of the curing agent concentration on the membrane permeability coefficients.

Another interesting perspective of this work could be to compare the designed chip with a chip built with a porous membrane. Such a chip would be characterized by the presence of a vapour–liquid interface. Therefore, its operation might be significantly different from the one of the chip designed in this paper.

Finally, continuous purification of  $\text{H}_2\text{O}_2$  in microdevices opens new perspectives of research, as it can be hazardous in batch processes.

## Acknowledgements

We acknowledge Dr. Pierre Miquel and Dr. Jean-Baptiste Salmon for helpful discussions, Prof. Michel Luhmer and Dr. Luca Fusaro for training at NMR and help with the optimization of NMR analysis, Dr. Alexandre Olive for his help with the first NMR analysis, Dr. David Mikaelian for his contribution to the numerical part of this work and Hervé Baudine for technical support. We thank the Solvay Company for its input in this project and the Brussels and Walloon regions for financial support through the WBGreen-MicroEco project. B.S. thanks the F.R.S.-FNRS for financial support as well as the Belgian Science Policy Office under the IAP 7/38 MicroMAST project. This work has been performed under the umbrella of the COST action MP1106.

## Notes and references

- 1 S. Bloomfield and P. M. Dhaese, WO2013135491 A1, 2013.
- 2 T. Inoue, Y. Kikutani, S. Hamakawa, K. Mawatari, F. Mizukami and T. Kitamori, *Chem. Eng. J.*, 2010, **160**, 909–914.
- 3 T. Inoue, K. Ohtaki, J. Adachi, M. Lu and S. Murakami, *Catal. Today*, 2014, DOI: 10.1016/j.cattod.2014.03.065.
- 4 S. A. Ahmad and S. R. Lone, *International Journal of Scientific & Engineering Research*, 2012, **3**, 1–5, ISSN 2229–5518.
- 5 L. Daubersies, J. Leng and J.-B. Salmon, *Lab Chip*, 2013, **13**, 910–919.
- 6 J. Leng, B. Lonetti, P. Tabeling, M. Joanicot and A. Ajdari, *Phys. Rev. Lett.*, 2006, **96**, 084503.
- 7 R. L. Hartman, H. R. Sahoo, B. C. Yen and K. F. Jensen, *Lab Chip*, 2009, **9**, 1843–1849.
- 8 Y. P. Zhang, S. Kato and T. Anazawa, *Lab Chip*, 2010, **10**, 899–908.
- 9 C. Adiche and K. Sundmacher, *Chem. Eng. Process.*, 2010, **49**, 425–434.
- 10 J. de Jong, R. G. H. Lammertink and M. Wessling, *Lab Chip*, 2006, **6**, 1125–1139.
- 11 J. N. Lee, C. Park and G. M. Whitesides, *Anal. Chem.*, 2003, **75**, 6544–6554.
- 12 C.-M. Bell, F. J. Gerber and H. Strathmann, *J. Membr. Sci.*, 1988, **36**, 315–329.
- 13 S. Wu, *et al.*, *Catal. Today*, 2000, **56**, 113–129.
- 14 N. A. Stephenson and A. T. Bell, *Anal. Bioanal. Chem.*, 2005, **381**, 1289–1293.
- 15 N. A. Lange and G. M. Forker, *Lange's Handbook of Chemistry*, McGraw, 1967.
- 16 J. J. van Laar, *Z. Phys. Chem.*, 1910, **72**, 723.
- 17 F. O. Rice and O. M. Reiff, *J. Phys. Chem.*, 1926, **31**, 1352–1356.
- 18 W. C. Schumb, *Ind. Eng. Chem.*, 1949, **41**, 992–1003.
- 19 E. J. Doedel, *Auto07p continuation and bifurcation software for ordinary differential equations*, Montreal Concordia University, 2008.